AGU PUBLICATIONS

JGR

Journal of Geophysical Research: Solid Earth

RESEARCH ARTICLE
10.1002/2016JB013596

Key Points:
- Thermoluminescence sensitivity increases with age for basalts from the eastern Snake River Plain, Idaho
- The correlation improves when a correction is applied for the compositional variations
- Further studies of the induced thermoluminescence of these basalt samples will yield new insights into their crystallization history

Correspondence to:
D. W. G. Sears,
derek.sears@nasa.gov

Citation:
Sears, D. W. G., H. Sears, A. Sehlke, and S. S. Hughes (2017), Induced thermoluminescence as a method for dating recent volcanism: Eastern Snake River Plain, Idaho, USA, *J. Geophys. Res. Solid Earth*, *122*, 906–922, doi:10.1002/2016JB013596.

Received 29 SEP 2016
Accepted 24 JAN 2017
Accepted article online 26 JAN 2017
Published online 8 FEB 2017

Induced thermoluminescence as a method for dating recent volcanism: Eastern Snake River Plain, Idaho, USA

Derek W. G. Sears[1], Hazel Sears[1], Alexander Sehlke[2], and Scott S. Hughes[3]

[1]NASA Ames Research Center, Bay Area Environmental Research Institute, Mountain View, California, USA, [2]NASA Ames Research Center, Mountain View, California, USA, [3]Geosciences Department, Idaho State University, Pocatello, Idaho, USA

Abstract The induced thermoluminescence properties of 24 samples of basalts from volcanoes in the eastern Snake River Plain, Idaho, were measured as part of an investigation into the possibility of using this technique for dating purposes. The volcanic flows sampled ranged in age from 2200 years to ~400,000 years. The thermoluminescence (TL) sensitivity values obtained, i.e., maximum induced TL normalized to that of the Dhajala meteorite (where Dhajala = 1000), ranged from 1.6 ± 0.3 to 226 ± 15 and showed a correlation between log TL and age with an r^2 value of 0.47. Thus, TL sensitivity values correlate with age in the manner expected, although there is a high level of scatter. We discuss various mechanisms for the correlation and scatter, particularly (1) the role of primary (igneous processes) and secondary (solid state processes), (2) composition of the plagioclase feldspar, and (3) weathering. The induced TL signal from feldspars, the mineral responsible for the TL, is strongly dependent on their composition, and correcting for this improved the correlation ($r^2 = 0.7$). Variations in primary feldspar are affecting the data, but we find no evidence that weathering of the samples is important. Further work is required to explore the remaining causes for the scatter and the TL-age trend. However, it is clear from the present study that induced TL has the potential for dating volcanism on the 2200 to 400,000 year time frame. This dating method, if successful, would be well-suited to spacecraft use since it requires low mass and low power instruments with a low data demand.

1. Introduction

May [1977, 1979] showed existing trends between ages in both the natural and the induced thermoluminescence for alkali basalts from the Big Island of Hawaii. Thermoluminescence (TL) is the light emitted as a sample is heated. It results from electrons in metastable excited states in a crystal lattice being released by thermal excitation. The natural TL is that which is observed from the "as-received" sample, while the induced TL is the signal produced by removing the natural signal and exposing the sample to a standard laboratory dose of ionizing radiation. Measurements of natural TL, or variants, are now in routine use for pottery dating [*Aitken*, 1985], personnel dosimetry [*McKinlay*, 1981], and dating quaternary sediments [*Aitken*, 1999]. In the geosciences, the natural TL dating technique was used by *Sutton* [1985] to date Meteor Crater. The calculated age based on this method was 50,000 years, which is twice the poorer age estimate based on sediment thickness [*Shoemaker*, 1983].

May [1977, 1979] applied the pottery dating techniques to the Hawaii basalts and reported ages that agree reasonably well with the isotopic ages. However, *Wintle* [1973] reported that volcanic feldspars are unreliable chronometers because they "leak" the signal. She referred to the process as "anomalous fading." This process is assumed to be due to the finite overlap of the wave functions for electrons in the ground and excited states [*Visocekas*, 1985], although other mechanisms have been proposed [*Templer*, 1986]. As a result of this, most workers dispute the value of natural TL as a dating technique for volcanic rocks, although several authors, like *May* [1977, 1979], have claimed a degree of success [e.g., *Guérin and Valladas*, 1980; *Berger*, 1991]. A number of means to circumvent anomalous fading have been proposed [e.g., *Fattahi and Stokes*, 2003; *Pilleyre et al.*, 1992] but, despite this, volcanologists have not embraced the TL dating of basalts.

It is the observation of May that the "artificial" TL, here called the "induced" TL, correlates with age that prompted the present study (Figure 1). May observed just over an order of magnitude increase in induced TL over about 200,000 years. The induced TL reflects the nature and amount of luminescent material in the rock and has been proven of great value in deciphering the thermal history of meteorites and lunar

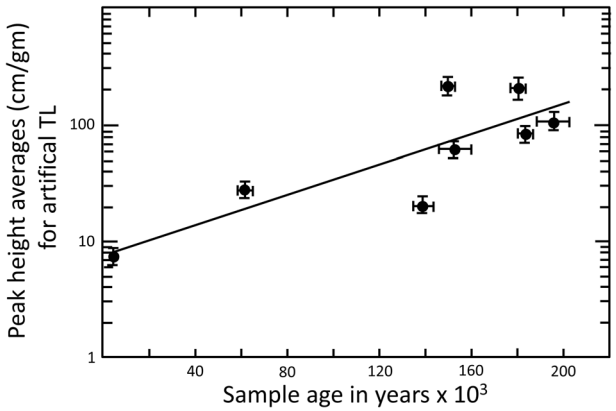

Figure 1. A simplified version of Figure 5 from the paper of *May* [1977] showing how the "artificial TL" (herein called the "induced TL") increases with the age of the alkali basalts from Hawaii. The induced TL increases by about an order of magnitude over ~200,000 years. May's Figure 5 was simplified by removing the natural TL data and the sample identifications.

samples [*Sears et al*., 2013]. *Sears et al*. [1980] first reported that the induced TL of the largest class of meteorites, the ordinary chondrites, increased by a factor of 10^5 as a result of metamorphism on their parent body. The subdivision of chondrites that resulted from this study is now part of the established classification protocol for these meteorites. The mechanism responsible is that the feldspathic elements in the original meteorites are in the form of a nonluminescent glass, but with time and metamorphism, this is converted to crystalline feldspar and this increases the induced TL to higher values.

Quite a different situation is found in the basaltic meteorites, the eucrites, now thought to originate with the closely related diogenites and howardites, on the asteroid Vesta [*Drake*, 2001; *McSween et al*., 2013]. In this case, a 100-fold increase in induced TL correlates with metamorphism as inferred by the compositional heterogeneity of the pyroxenes in the meteorites [*Batchelor and Sears*, 1991a]. However, this increase in induced TL is because the feldspar in unmetamorphosed eucrites contains Fe, a well-known quencher of luminescence, which diffuses out of the feldspar with increasing metamorphism [*Batchelor and Sears*, 1991b]. Thus, we have two mechanisms that could explain the *May* [1977, 1979] observation that induced TL increases with age, crystallization of the glass, and the diffusion of Fe out of the plagioclase. These mechanisms have been discussed in more detail by *Sears* [2015].

We decided to determine whether another volcanic province with volcanism in the same age range as the Big Island of Hawaii also showed a trend of increasing induced TL with age. The eastern Snake River Plain, Idaho, is a popular planetary analog site and the prime example of "plains volcanism" [*Greeley*, 1982]. This category of volcanism was first described by Greeley, although others had noted the unusual volcanism of the Snake River Plain. He described it as intermediate between basaltic flood (or plateau) eruptions and Hawaiian volcanism. Like Hawaiian volcanism, plain volcanism multiple flows, generally from a point source, formation of low shields and frequent use of lava tubes and channels. Like flood basalts, plain volcanism involves high volumes of magma, vents along rift zones and planar surfaces. At the heart of the volcanic area in Idaho is the Craters of the Moon National Monument and Preserve. The region has been described in some detail by Greeley and his colleagues [*Greeley and King*, 1977] and by Kuntz and his colleagues [*Kuntz*, 1992]. Their work was summarized and the volcanism further described in a field guide by *Hughes et al*. [1999]. The Greeley studies focused particularly on the value of the site as an analog of volcanism observed on the Moon and Mars which lack plate tectonics. Because of its analog value, in addition to a NASA workshop [*Greeley and King*, 1977], the lava fields of Idaho have been used for astronaut training [*NPS*, 2015] and were chosen as a site for the NASA FINESSE project (Field Investigations to Enable Solar System Science and Exploration, principal investigator Jennifer Heldmann) [*Heldmann et al*., 2015], which is part of NASA's Solar System Exploration Research Virtual Institute.

2. Experimental Methods

2.1. Sample Collection

The sites at which samples were collected are identified in Figure 2 and are listed, along with their ages, in Table 1. Descriptions of the site and the rocks at that site for most of our samples can be found in *Kuntz et al*. [2007]. Clean interior samples were removed from outcrops by using a sledge hammer. We went to some effort to collect samples from the same sites as previous workers, and in several instances, we could identify precisely the sites of previous sampling from outcrop damage. However, in other

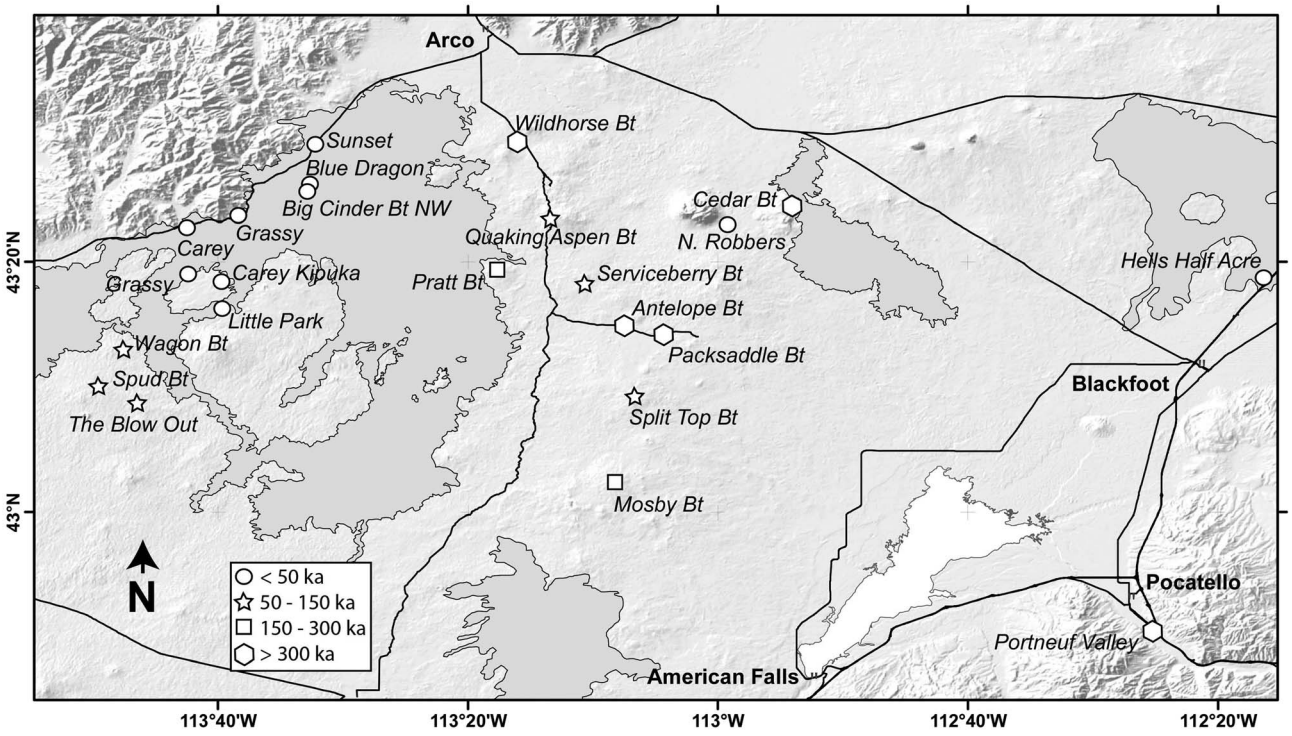

Figure 2. Map of part if the eastern Snake River Plain in Idaho, which includes Craters of the Moon National Monument and Preserve, showing the locations at which the samples were taken for this study and their age (see inset key) as determined by radiocarbon and K-Ar methods. Bt = Butte.

Table 1. Samples Used in the Present Study, Their Ages, and References (in Order of Increasing Age)

Volcano	Longitude (W)	Latitude (N)	Map Unit[a]	Abb[b]	Age (ka)[c]	Ref.[d]
Blue Dragon Flow	113.544067	43.435433	Qcfa2	BLU	2.076 ± 0.045	a, b
Hell's Half Acre	112.272716	43.302287	Qba	HHA	5.2 ± 0.15	b, d
Big Cinder Butte NW	113.547767	43.427367	Qcfc4	BCB	6.02 ± 0.16	a
Little Park Flow	113.660250	43.272267	Qcfd3	LPT	6.5 ± 0.06	a, b
Carey Kipuka Flow	113.664333	43.308250	Qcfd2	CKF	6.6 ± 0.06	a, b
Grassy A	113.704817	43.316283	Qcfe1	GRA	7.36 ± 0.06	a, b
Grassy B	113.639217	43.391800	Qcfe1	GRF	7.36 ± 0.06	a, b
North Robbers	113.987700	43.382200	Qba	NOR	11.6 ± 0.3	b, d
Carey Flow	113.709600	43.381650	Qcfg2	CAR	12.01 ± 0.15	a, b
Sunset	113.536517	43.489633	Qcfg1	SUN	12.01 ± 0.15	a
Spud Butte	113.825500	43.168950	Qsbb7	SPU	57 ± 30	a, b
Quaking Aspen Butte	113.223400	43.388083	Qsbb19	QUA	64 ± 20	b
Split Top Butte	113.112733	43.153217	Qsbb28	SPL	113 ± 10	a, b
Wagon Butte	113.792567	43.214250	Qsbb13	WAG	120 ± 25	a
The Blowout	113.775850	43.133350	Qsbb11	BLO	116 ± 15	a, b
Serviceberry Butte	113.178933	43.303567	Qsbb22	SER	120 ± 12	a, b
Pratt Butte	113.296633	43.322950	Qsbc35	PRA	263 ± 20	a, b
Mosby Butte	113.136117	43.038017	Qsbc52	MOS	265 ± 30	a, b
Packsaddle Butte	113.071933	43.234517	Qsbc63	PAC	340 ± 15	a
Cedar Butte	113.896900	43.404050	Qbd	CED	400 ± 19	b
Portneuf Valley	113.418283	42.838133	Qp	PNV	430 ± 70	c
Antelope Butte	113.128267	43.247017	Qsbd5	ANT	470 ± 25	a

[a]Geological unit according to *Kuntz et al.* [2004, 2007].
[b]Abbreviation used in the figures.
[c]Ages less than 50 ka are radiocarbon ages; ages >50 are K-Ar ages.
[d]References: a, *Kuntz et al.* [2007]; b, *Kuntz et al.* [2004]; c, *Rodgers et al.* [2006]; d, *Kuntz et al.* [1986].

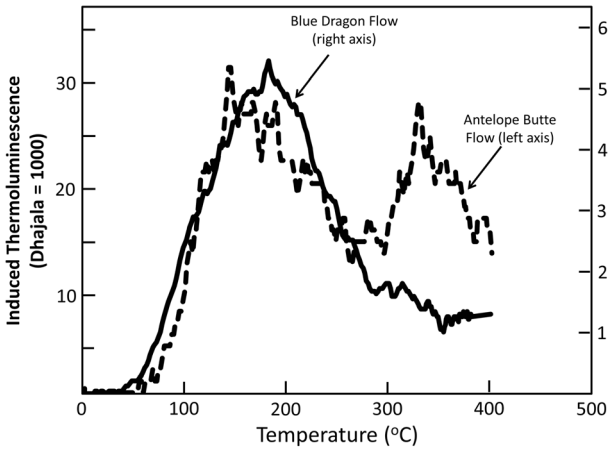

Figure 3. Representative glow curves, plots of thermoluminescence against heating temperature, for two of the present samples. The solid line is for the Blue Dragon Flow basalt (2.076 ± 0.045 ka), while the broken line is for the Antelope Butte basalt (470 ± 25 ka).

instances, while we were confident that we were at the same sites, we could not be sure. Thus, there is a concern that the compositional data and present data may be for samples from different locations. We return to this below.

2.2. Sample Preparation

In the laboratory, under red light, the samples were crushed in stainless steel and agate pestles and mortars and the powder that passed through a 200 μm sieve was used for the TL measurement. No further processing, such as mineral separations, was performed since experience shows that this introduces more scatter than it removes [*Sears and Durrani*, 1978]. Four milligram aliquots were placed in 5 mm diameter, 0.25 mm deep, copper pans. This procedure is designed to produce a monolayer of grains.

2.3. Thermoluminescence Sample Runs

A modified Daybreak Nuclear and Medical Inc. thermoluminescence apparatus heated the samples to 500°C at a rate of 7.5°C/s during which the light produced is measured as a function of heating temperature. The apparatus used a nichrome heating strip in an oven that has been evacuated to ~100 torr and filled with nitrogen flowing at a rate sufficient to maintain a pressure about 10% higher than atmospheric. The light detection system was an 9635QB photomultiplier tube with a gain of 10^9 specially developed for TL applications. A heat filter and a blue filter were placed in front of the photomultiplier tube, which was located in a housing cooled by a Peltier effect system. The tube was also surrounded by a magnetic shield, and the housing is equipped with a shutter so that the 1000 V power supply was never switched off. This enhances stability. A sample of the Dhajala meteorite was run to monitor the stability of the equipment and act as a normalization standard. The data were digitally collected, and the resulting plot of light against temperature is referred to as the "glow curve" (Figure 3). After the first heating, during which the stored natural TL signal was removed, the samples were irradiated with a 150 mCi ^{90}Sr beta source for 3 min and the TL induced was measured. The induced TL measurement was repeated three times. Finally, the signal from the drained sample was also measured so as to record background and blackbody radiation.

2.4. Thermoluminescence Data Reduction and Terms

Thus, for each sample, there are five glow curves, one for the natural sample, three for irradiated samples, and one background/blackbody. The quoted uncertainties are the standard deviations shown by the three replicates. We refer to the glow curves we obtain as describing the natural TL, induced TL, and blackbody. In order to quantify the curves we measure the intensity at the maximum and divide this by the maximum intensity of the induced TL from the Dhajala meteorite. We refer to this as the "TL sensitivity." For low intensity samples, like the present samples, we quote the units of Dhajala = 1000. When trying to detect variations in one part of the glow curve we sometimes measure peak-height ratios. We also note the temperatures of apparent peaks as the sample is heated in the apparatus and inflections in the glow curves that reflect unresolved peaks.

2.5. Petrography

In order to better understand the crystallization histories of the samples, and thus the induced TL behavior, we prepared polished thin sections and examined the samples in plane and cross-polarized lights by using a Leitz Orthoplan polarizing microscope. Several images of the thin sections were taken with a camera attached to the microscope. We noted trends by visual inspection and by quantifying components in the samples by counting the number of pixels corresponding to each phase (plagioclase, olivine, and glass).

Table 2. Thermoluminescence Data for the Present Samples[a] (in Order of Increasing Age)

	TL Sensitivity[b]	Peak Positions (°C)[c]					
	(Dhajala = 1000)	1	2	3	4	5	HT/LT[d]
Blue Dragon Flow	4.5 ± 0.9	118	180	207			0.26 ± 0.02
Hell's Half Acre	1.5 ± 0.3	110		205			1.00 ± 0.10
Big Cinder Butte NW	7.0 ± 1.8	118	165	200		330	0.65 ± 0.07
Little Park Flow	12.5 ± 2.5	125		213		285	0.29 ± 0.02
Carey Kipuka Flow	8.8 ± 1.0	133		203		323	0.74 ± 0.07
Grassy A	23.5 ± 10.3	128	163	195	270	320	0.71 ± 0.21
Grassy B	7.0 ± 2.6	120		193		325	0.23 ± 0.10
North Robbers	81.0 ± 1.7	125		215			1.07 ± 0.18
Carey Flow	5.8 ± 2.8	108	169				0.38 ± 0.09
Sunset	12.3 ± 3.2	120		190			0.92 ± 0.13
Spud Butte	55.3 ± 3.1	125	160	197		323	1.04 ± 0.24
Quaking Aspen Butte	4.3 ± 0.6	120	155	220		3232	1.93 ± 0.47
Split Top Butte	15.3 ± 5.3	145	168	200	225	313	0.63 ± 0.03
Wagon Butte	53.3 ± 7.6	128	173	198		305	0.25 ± 0.01
The Blowout	61.7 ± 16.1	115					0.19 ± 0.06
Serviceberry Butte	17.5 ± 2.2	120	175	212		318	0.44 ± 0.05
Pratt Butte	17.3 ± 2.5	123	158	200	245	320	0.65 ± 0.02
Mosby Butte	14.3 ± 5.3	128		198	240	330	0.97 ± 0.23
Packsaddle Butte	28.7 ± 5.0	115		202		333	1.48 ± 0.12
Portneuf Valley	226.0 ± 15.1	125		200		312	0.35 ± 0.02
Cedar Butte	6.6 ± 0.5	128	163	198	250	315	0.13 ± 0.04
Antelope Butte	31.3 ± 6.4	120		195	230	320	0.59 ± 0.08

[a]Uncertainties are standard deviations based on triplicate measurements.
[b]"TL sensitivity" is defined as the maximum induced TL level divided by the same value for the Dhajala meteorite.
[c]Positions of peaks or inflections in the TL glow curves indicative of unresolved peaks. Uncertainties on the peak positions can be visually estimated from Figure 3 and are typically ±10°C at the 1 sigma level.
[d]Ratio of the induced TL at ~325°C to ~125°C.

The histogram function of Adobe Photoshop® and plane polarized transmitted light images were used for this purpose. Modes were calculated after correcting for vesicles.

2.6. Geochemistry

Compositions of the samples were obtained from a database maintained by one of the authors (S.S.H.). Most of the analyses were reported by *Kuntz et al*. [1992] and *Staires* [2008]. CIPW norms were calculated from the data.

3. Results

3.1. Thermoluminescence Results

The TL sensitivity for these samples is listed in Table 2. The TL sensitivities range from 1.5 ± 0.3 to 226 ± 15.1, a factor of 150. These intensities are quite low (meteorites range from 3 to 22,000 on this scale), which is reflected in the relatively large uncertainties for the present samples of 5% to 50%, but typically ~20%. However, given the total range, these errors are not problematic and scatter will be discussed later.

Given that we know little about the stability of the TL signal in these materials, at the suggestion of Steve Sutton, we examined the data for individual triplicates (Figure 4). If the heating required to read out the TL signal (or the irradiation step) caused changes in the sample, then we might see the signal increase from the first to the second and third measurements. In fact, we do not, and it seems that the measurement procedure does not significantly affect the TL of the samples. We do note, in passing, that the TL-age trend is present in the raw data in Figure 4, which plots the samples in order of increasing age.

Figure 5 plots the TL sensitivity (on a logarithmic scale) against the radiocarbon or K-Ar age by using data and sample abbreviations in Tables 1 and 2. The line through the data is a regression line which suggests that the induced TL increases by about an order of magnitude in ~500 ka. However, there is also considerable scatter. There is about an order of magnitude scatter among the $<$20 ka samples (more including the HHA outlier),

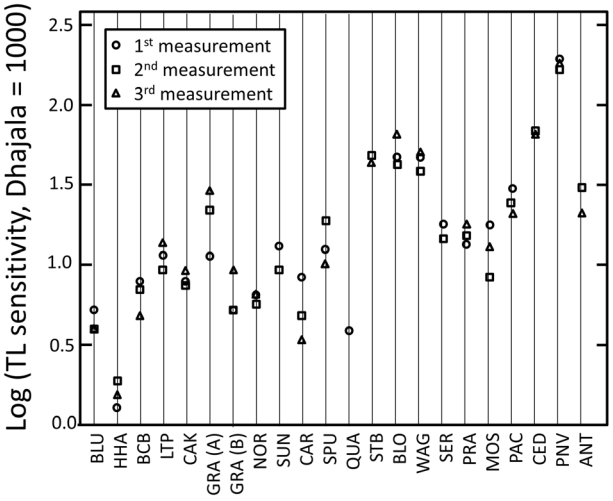

Figure 4. Testing whether the heating and irradiation are necessary to read out the induced TL is affecting the data. There is no evidence that values increase (or decrease) with order of measurement. Samples are plotted in order of increasing age, and sample abbreviations are given in Table 1.

and Antelope Butte (whose age is ~470 ka) is about an order of magnitude lower in TL sensitivity than the Portneuf Valley whose age is similar (~430 ka).

There is no model to predict the form of the relationship between TL sensitivity and age, and for Figure 5, we use the simplest option, namely, a linear fit, following *May*'s [1977, 1979] example. More complex trend lines were tried and did not produce a better fit, not a surprise given the scatter on the data. However, we see no justification for assuming a more complex fit until we have a better understanding of the eruption and crystallization behavior of these basalts and of the kinetics of the various equilibration processes. This is among the work planned.

Glow curves representing the extremes of those observed are shown in Figure 3; most were intermediate to these two curves. The Blue Dragon Flow consists of a peak in the 100–200°C region of the glow curve, whereas Antelope Butte has an additional peak, almost as strong, in the 200–400°C region. In Table 2 we list our observed peak positions, or positions of inflections suggesting the presence of peaks, and in Figure 6, we plot these data. This figure demonstrates the persistence of peaks at 100 and 200°C which often overlap, producing a band between 100 and 200°C. There is also a third peak at ~325°C. There are sometimes peaks at ~160°C and ~225–270°C, but in view of their absence in many curves and the possibility that they result from peak overlap, we will focus on the three major peaks (~125°C, ~200°C, and ~325°C). The variety of curves we observed is very similar to those observed by *May* [1977, 1979] in his studies of Hawaii basalts. He suggested that there were four peaks in the glow curves. It is clear that these peaks, perhaps better termed "bands," are in fact composites of many individual peaks so that the exact peak temperature depends on overlap and intensity. The ratio of the induced TL at ~325°C to that at ~200°C shows no significant pattern with the age of the samples.

3.2. Petrographic Results

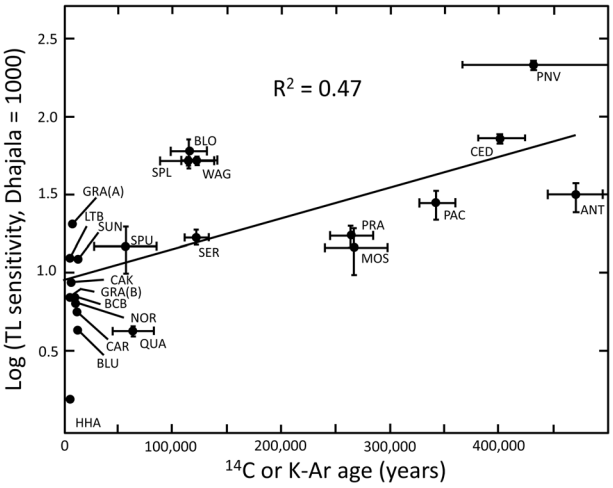

Figure 5. Thermoluminescence sensitivity of the basalt samples shown in Figure 2 plotted against their radiocarbon or K-Ar ages. The line is a regression line ($n = 23$, $r^2 = 0.47$). Samples are identified in Table 1.

The microphotographs of four of our samples, chosen to represent a variety of ages, are shown in Figure 7. These include the two samples whose TL glow curves were shown in Figure 3. In general, the basalts consist of an opaque glass, or amorphous phase, with lathes of feldspar in the form of microlites of phenocrysts and small amounts of a mafic phase, usually olivine. The youngest sample in Figure 7 is the Blue Dragon Flow (Figure 7a), with an age of 2 ka and induced TL of 4.5, consisting mostly of glass with several vesicles and an occasional small feldspar microlite. The next sample in Figure 7 is Sunset Butte (Figure 7b), which has an age of 12 ka and induced TL of 12.3, and in section is seen to be abundant

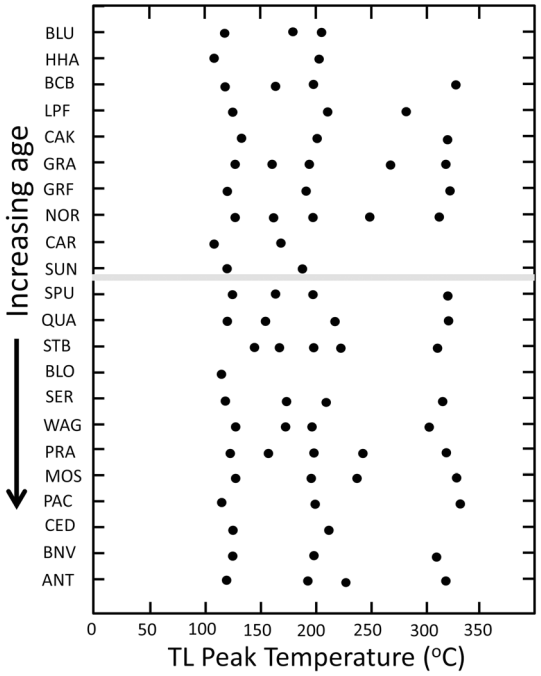

Figure 6. The position of peaks or inflections (inferring unresolved peaks) in the induced TL glow curve. Three, four, or even five peaks appear to be present, but the most resilient seem to be the peaks at ~125°C, ~200°C, and ~325°C. A peak at 160°C is present in about half the samples, and in a few, there is a peak at ~225°C.

glasswith numerous small lathes of feldspar microlites. The third sample (Serviceberry Butte, Figure 7c), with an age of 120 ka and induced TL of 17.5, has considerably less glass, although significant glass is still present but numerous large phenocrysts of feldspar. The last sample in Figure 7 (Antelope Butte, Figure 7d) has an age of 470 ka and induced TL of 31.3 and consists of large crystals of feldspar with abundant smaller crystals of olivine and a largely finely crystalline mesostasis.

We summarize the petrographic observations for all our sections in Figure 8 where we display the images in the same pattern as the induced TL versus age plot (Figure 5). Two observations can be made. First, the trend we see in the four examples in Figure 7 is borne out by the remaining samples. The images lighten up as one proceeds from bottom left to top right reflecting the loss of the glassy or amorphous phase, which appears black in these images, and the gain of crystalline material, the lighter phase. Second, the large range of induced TL is shown by the young samples in Figure 8 which appear to be petrographically very similar and consist predominantly of opaque glass with numerous vesicles.

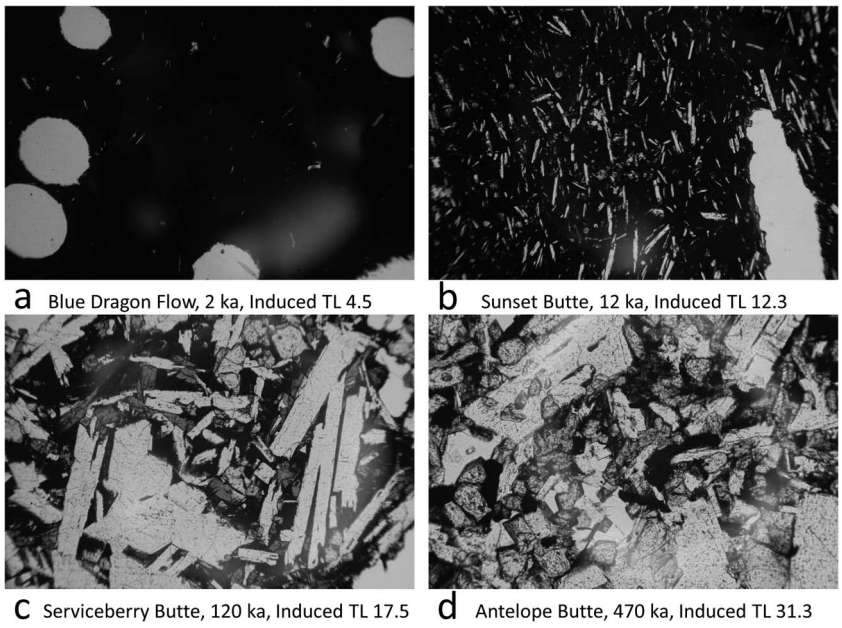

Figure 7. Photomicrographs in plane polarized light of four basalts from the present study photographed under transmitted light. Field of view 0.5 cm. With increasing age and induced TL the amount of opaque glass (amorphous phase) decreases and the amount of crystalline material, mostly feldspar (bright), increases. Several large vesicles can be seen in the Blue Dragon basalt, and olivine grains (brown/midgray) can be seen in the Antelope Butte basalt.

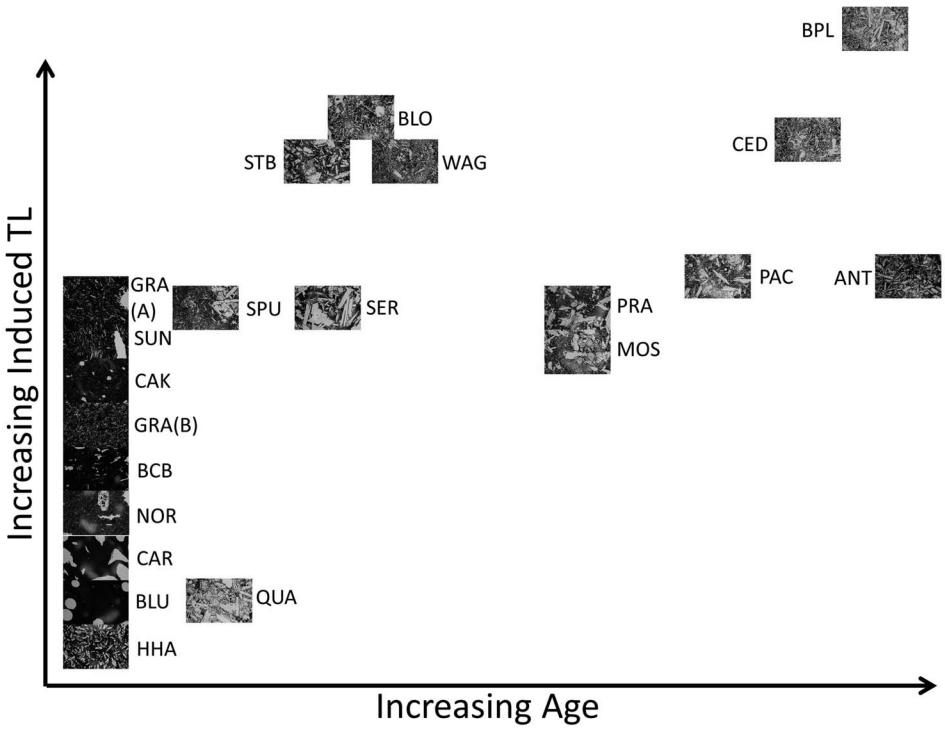

Figure 8. Photomicrophotographs in plane polarized light of the basalts from Craters of the Moon and surrounding areas laid out in the pattern of the induced TL versus age plot (Figure 5). The images show that the opaque phase is replaced with crystalline phases with increasing age and induced TL, but the low-age samples show a very wide range in induced TL.

Table 3. Modal Abundance (vol %) of Plagioclase Phenocrysts, Plagioclase Microlites, Olivine, and Glass as Determined by Image Analysis of Transmitted Light Photo Micrographs (in Order of Increasing Age)

	$Plag_{pheno}$	$Plag_{micro}$	Olivine	Glass
Blue Dragon Flow	14	0	0	86
Hell's Half Acre	0	23	14	64
Big Cinder Butte	0	7	0	93
Little Park Flow	0	8	0	92
Carey Kipuka	0	13	0	87
Grassy A	0	12	0	88
Grassy B	0	23	0	77
North Robbers	12	41	9	38
Carey Flow	0	0	0	100
Sunset	0	9	0	91
Spud Butte	14	33	6	48
Quaking Aspen Butte	45	0	35	20
Split Top Butte	5	42	21	32
Split Top Butte 2	3	42	23	32
Wagon Butte	26	16	13	45
The Blowout	0	42	22	36
Serviceberry Butte	46	0	19	36
Pratt Butte	30	10	16	44
Mosby Butte	28	21	13	38
Packsaddle Butte	16	26	10	48
Portneuf Valley	45	0	35	20
Cedar Butte	6	29	0	65
Antelope Butte	25	0	26	48

Table 3 shows the results of our modal analysis. Opaque phases and vesicles were also determined and removed from the analysis since we were mainly interested in the plagioclase-glass-olivine relations. We report a standard uncertainty of at least 5 vol % on these estimates, based on variations in color tolerance used to count the pixels of each phase. Plagioclase phenocrysts were absent in many samples but reached as high as 46 vol % in others. Similarly, plagioclase microlites were absent in many samples but could reach as high as 42 vol %. Olivine reached as much as 35 vol % but was absent in nine samples. Glass was present in all our basalts, reaching 100 vol % in Carey Flow and falling to 20 vol % in Portneuf Valley and Quaking Aspen Butte. Figure 9 shows these data graphically plotted in order of increasing age. A grey vertical bar separates the samples with $<$20 ka age from the older samples. In general, the younger samples have fewer phenocrysts, less olivine, and

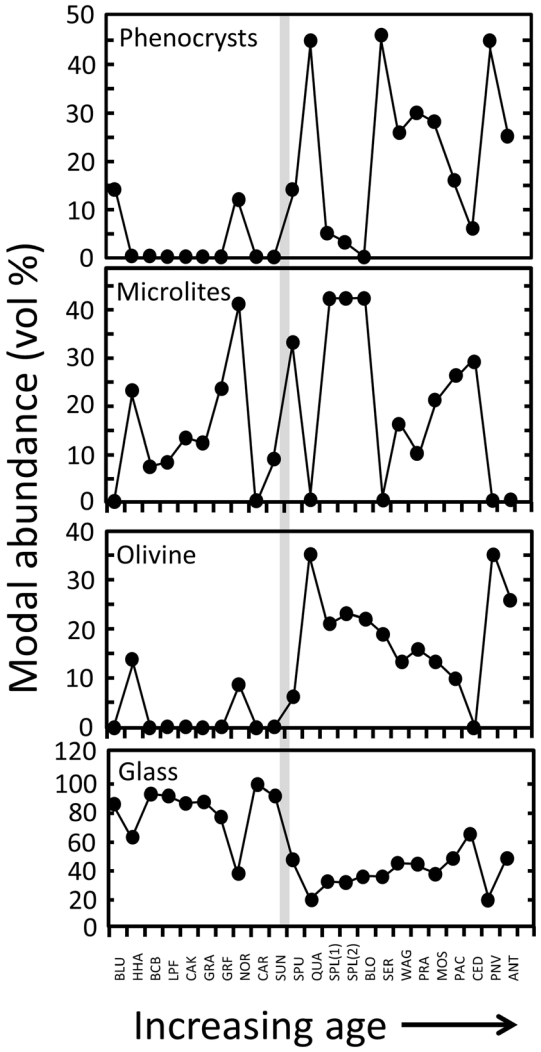

Figure 9. Vesicle-corrected modal abundances of phenocrysts, microlites, olivine, and glass in the present samples, plotted in order of increasing age. The grey vertical bar separates the <20 ka samples (to the left) from the >20 ka samples.

more glass. The microlite abundance is highly variable but not significantly different for the younger and older samples.

3.3. Bulk Compositions

The bulk compositions of the present samples are listed in Table 4 along with expected equilibrium plagioclase (anorthite values) composition determined from the CIPW norm. The compositions are plotted in a total alkali-silica plot in Figure 10. Most of our samples are basalts, or basalt-like, although two (Cedar Butte and Antelope Butte) are considerably higher in alkalis and silica and plot in the trachydacite field. The spread in alkalis in the basalt-like samples is significant, 3 wt % to 8 wt %, since induced TL is so heavily dependent on feldspar composition. The normative anorthite composition also shows a large range, 23.49 mol % (Sunset Butte) to 63.43 mol % (Quaking Aspen Butte) lava flows with an average of 48 mol %.

4. Discussion

4.1. TL Sensitivity and Age

First, we confirm *May*'s [1977] observation of a correlation between TL sensitivity and age for volcanic samples. Our hypothesis going into this project was that the nonequilibrium system produced during flow and crystallization of these lavas would move to equilibrium over time and the induced TL would increase [*Sears*, 2015]. The precise mechanism would be a mixture of the crystallization of glass and the diffusion of incompatible elements out of the feldspar, the mineral responsible for the TL. These processes are observed in chondritic meteorites and basaltic meteorites. The opposite process is observed for the lunar regolith where long-term regolith working, mostly by micrometeorite bombardment, converts the crystalline feldspar to glass and the induced TL goes down with time [*Benoit et al*., 1996]. Similarly, heavily shocked equilibrated meteorites can drop in induced TL as the residual temperatures from the shock compression convert feldspar to glass [*Haq et al*., 1988; *Hartmetz et al*., 1986]. One of our objectives in our discussion is to explain the correlation we observe here for the Idaho volcanic rocks between TL sensitivity and age.

However, there is considerable scatter in the data which must be understood and the effects removed before we can claim that TL sensitivity is a useful chronometer. The major potential causes of scatter that we have identified and will discuss are differences in (1) the amount of "primary" and "secondary" feldspars, (2) feldspar composition, and (3) the weathering suffered by the sample.

4.2. Differences in the Amount of "Primary" and "Secondary" Feldspars

We take it as a given that the thermoluminescence produced by basalts is due to the crystalline feldspar they contain. Feldspar is the brightest of the common rock-forming minerals, by a factor of 13 or more [*Lalou et al*.,

Table 4. Bulk Composition of the Present Basalts, Where Available, and the CIPW Normative Anorthite in the Plagioclase (mol %)[a] (in Order of Increasing Age)

Flow Group or Type	SiO_2	TiO_2	Al_2O_3	FeO[b]	MnO	MgO	CaO	Na_2O	K_2O	P_2O_5	An
Blue Dragon Flow	49.23	2.8	14.0	15.7	0.3	3.4	7.1	3.6	2.0	1.8	33.90
Hell's Half Acre	47.38	3.17	14.75	14.33	0.20	6.80	9.30	2.64	0.83	0.59	50.97
Big Cinder Butte NW[c]	63.7	0.68	14.67	8.47	0.17	0.27	2.98	4.25	4.70	0.14	15.55
Big Cinder Butte NW[c]	61.6	0.98	14.32	10.36	0.18	0.53	3.65	4.11	4.02	0.30	19.22
Little Park Flow	50.04	2.58	14.45	14.73	0.24	3.12	6.57	4.33	2.33	1.62	25.20
Carey Kipuka	51.07	2.45	14.31	14.42	0.22	2.98	6.35	4.33	2.41	1.48	51.80
Grassy Cone	48.28	3.30	12.76	15.53	0.26	3.90	8.58	3.14	1.86	2.38	35.15
North Robbers	46.71	2.20	15.45	12.40	0.18	9.04	10.45	2.54	0.42	0.62	56.44
Carey	47.41	3.10	13.51	15.78	0.26	3.93	8.27	3.48	1.95	2.30	33.00
Sunset Butte	49.96	2.46	14.59	14.63	0.24	3.16	6.51	4.53	2.36	1.57	23.49
Spud Butte	50.9	2.67	14.23	14.86	0.24	2.83	7.03	3.43	2.18	1.60	35.60
Quaking Aspen Butte	47.36	1.77	16.00	11.27	0.18	8.62	11.54	2.42	0.43	0.41	63.43
Split Top Butte	46.68	2.99	15.41	14.46	0.20	6.97	9.55	2.82	0.69	0.80	51.97
Wagon Butte	50.9	2.67	14.23	14.86	0.24	2.83	7.03	3.43	2.18	1.60	35.60
The Blowout	50.9	2.67	14.23	14.86	0.24	2.83	7.03	3.43	2.18	1.60	35.60
Serviceberry Butte	45.11	2.93	14.97	14.24	0.20	7.02	9.76	2.69	0.62	0.91	54.12
Pratt Butte[c]	44.15	2.88	13.83	13.89	0.20	6.75	11.26	2.38	0.77	1.01	53.70
Mosby Butte	44.15	2.88	13.83	13.89	0.20	6.75	11.26	2.38	0.77	1.01	53.70
Packsaddle Butte	45.23	2.55	14.83	13.30	0.19	7.73	10.19	2.40	0.48	0.65	56.70
Portneuf Valley	47.37	2.37	15.34	12.41	0.19	8.35	9.99	2.38	1.14	0.49	56.60
Cedar Butte	63.71	0.91	13.46	8.83	0.25	0.65	3.37	4.02	4.50	0.30	58.70
Antelope Butte	47.07	3.00	14.95	14.40	0.20	6.61	9.68	2.95	1.06	0.71	48.05

[a]Geochemical data, normalized to 100% volatile free and total Fe reported as FeO, from *Kuntz et al.* [1992] and *Staires* [2008].
[b]All Fe expressed as FeO.
[c]In these cases no analysis was available and a surrogate has been used. Big Cinder Butte = Highway Flow and Serrate Flow, Pratt Butte = Mosby Butte, Spud Butte = Broken Top Butte, The Blowout and Wagon Butte = Broken Top Butte.

1970], it is the major normative constituent of these basalts, has glow curve shapes similar to those of pure feldspars and catholuminescence images of basaltic and ultramafic meteorites, and lunar samples show that it is the feldspar that produces the major luminescence [*Akridge et al.*, 2004]. However, feldspars are complex minerals, varying in composition and structure, both of which affect TL properties. A considerable aid in interpreting the TL results and their mineralogical interpretation are measurements with pure feldspars [*Benoit et al.*, 2001] and interpretations developed from meteorite lunar sample observations [*Sears et al.*, 2013].

For our present purposes we can consider the feldspar in our samples to be of two kinds: (1) that which was present when the rock cooled to ambient temperatures and (2) that which formed after solidification and

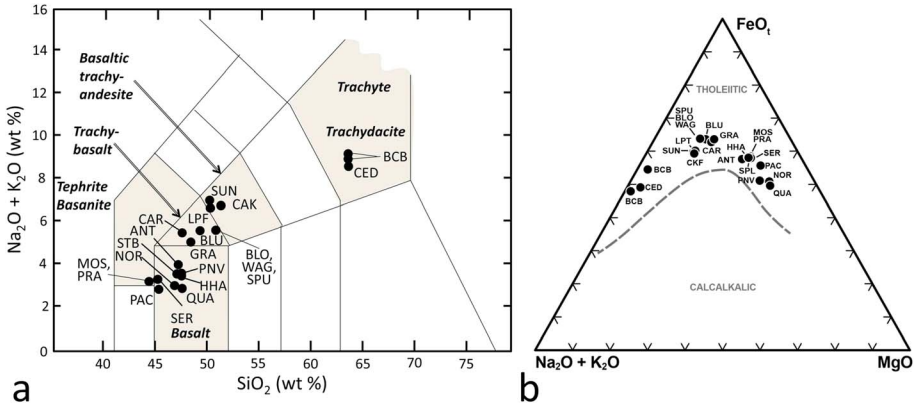

Figure 10. (a) The present compositional data plotted on a total alkali against silica plot. Most of the present samples are basalts, or basalt-like, although two are especially high in alkalis and silicon and appear in the trachydacite field. (b) Investigated East Snake River Plain bulk compositions plotted in an AFM discrimination diagram, dividing line for tholeiitic and calc-alkaline trends after *Irvine and Baragar* [1971].

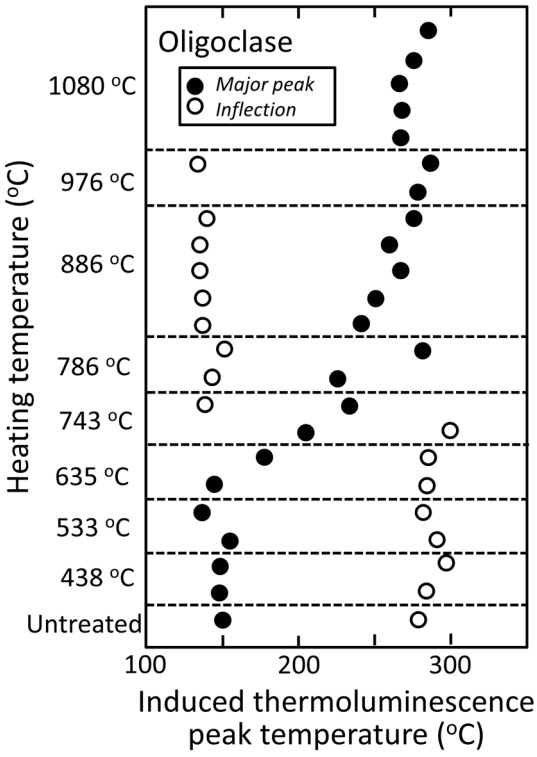

Figure 11. Plot of the induced TL peak temperature of bytownite, which resembles the normative composition of the plagioclase in tholeiites, after heating in a tube furnace at the temperatures indicated. X-ray diffraction studies indicate that this behavior is related to the transformation of low-temperature (ordered) feldspar to high-temperature (disordered) feldspar. In the 786°C sample, although the major peak was at ~240°C, a relic of the ~140°C peak could be seen as an inflection at ~160°C. This is indicated with the open symbol. Figure from *Benoit et al*. [2001].

cooling over the lifetime of the basalt. We refer to the first as "primary" and the second as "secondary." Primary feldspar consists of phenocrysts that may have been present before eruption and feldspar that formed by crystallization during the flow. Secondary feldspar either formed by the crystallization of glassy or amorphous phases or formed earlier but became luminescent by diffusive loss of iron from the feldspar. Since thermoluminescence detects all forms of feldspar, the simplest explanation for the age relationship would be that it is the result of the formation of secondary feldspar while the abundance of primary feldspar adds scatter to the data. However, as we will find, other explanations are possible.

The major complication is that we do not know the relative proportions of primary and secondary feldspars, although we can suggest possibilities. For instance, the amount of primary feldspar emerging from either a stratified magma chamber or volcanic conduit might vary with time during an eruption; it could be more abundant in the earliest lavas and would decrease in amount along the length of a flow since greater distances mean earlier flow from the vent. Alternatively, the abundance might decrease with time so that there is a stratigraphy with older, deeper, lavas having more primary feldspar than shallower and younger lavas. This is certainly true to some extent, as we discuss later (section 4.5). In this case, the scatter in our data may be due to sampling greater depths as the volcano ages.

Alternatively, the major source of primary feldspar might be due to crystallization during the flow of the lava. One expects systematic changes in the thermal history along a flow, such that a temperature decrease promotes in situ crystallization within the lava during emplacement. Thus, increasing amounts of primary feldspar are expected along a single flow, the opposite trend to that speculated above. This was observed and quantified in Hawaiian lava along a channelized lava flow by the study of *Robert et al*. [2014]. The sudden increase in microlites in the lava about 4 to 5 km away from the vent has been identified as the cause of a sudden increase in viscosity and thus a change in the surface texture and morphology of the flow. Thus, low microlite lavas generally have a lower viscosity and exhibit pahoehoe surface textures, while high-microlite lavas have higher viscosity with `a`a surface textures at the same strain rate [*Sehlke et al*., 2014]. In this case, the scatter in our data would be due to sampling different places in a flow with variable amounts of primary feldspar on each volcano. In the present case, the majority of our samples were taken close to the vent, so crystallization during flow should not be a major factor in scattering the TL data.

Perhaps some insights can be gained from TL evidence for the thermal history of our samples. Induced TL peak temperature depends on the thermal history of the feldspar [*Benoit et al*., 2001]. Figure 11 shows the results for oligoclase, but most plagioclases behave this way. In the oligoclase case, the peak remained at about 150°C in the glow curve until heating to 635°C in the furnace when it moved gradually to 300°C after heating to 866°C. The effects of the heat treatments on the feldspar were monitored by X-ray diffraction which showed that the heat treatments had caused the initially ordered feldspar to become disordered.

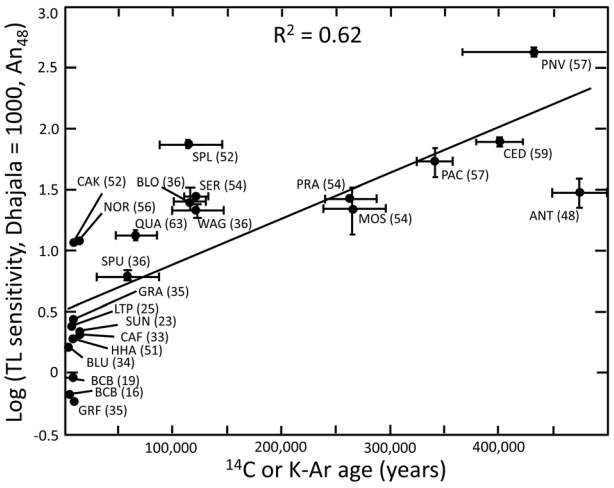

Figure 12. Logarithm of the induced TL corrected for compositional differences plotted against age. Compositional differences have been removed by normalizing to An_{48}, and the An values were calculated by using the CIPW norm program. The correlation is significantly improved by this correction. Also indicated are the normative An content of the plagioclase in mol % to two figures. Most of the young samples have low An (say 24–35), suggesting that the compositional correction has not fully removed the effect of differing plagioclase compositions.

The peaks observed in the present samples suggest that the present feldspar formed in both the ordered and disordered phases (Figure 3) without a systematic age correlation. We suggest that this relates to our sampling, whereby the samples collected from the vents consisted of primary feldspars that experienced a variety of thermal histories. The samples deposited near the vent would suffer a variety of thermal histories due to differences in burial under other flows and pyroclastics. This also, of course, would be a cause of scatter in our data. In contrast, the samples collected along a single flow might be expected to exhibit systematic changes in the induced TL peaks observed. In this case, a means of removing scatter would be to find a way of always sampling from the same region of a flow (e.g., same distance from the vent).

4.3. Differences in Feldspar Composition

We return now to feldspar composition, reiterating that TL sensitivity is strongly dependent on the composition of the feldspar. Fitting a regression line to *Benoit et al*. [2001, Figure 2] yields an equation (with $R^2 = 0.986$):

$$\text{Log (TL sens)} = -0.0316\,\text{An} + 4.3125 \quad (1)$$

where the induced TL is in units of Dhajala = 1000 and An is in mol %. We can therefore derive a correction factor that enables the induced TL of our samples to be normalized to a single An value, say An_{48}, that removes the compositional effects. The new plot of log (TL sensitivity, corrected to An_{48}) against isotopic age appears as Figure 12. The correlation is significantly improved ($R^2 = 0.62$), suggesting that the composition of the feldspar is the major cause of the scatter in Figure 5. The correlation might be improved further because compositional heterogeneity for a single volcano or flow can be contributing some uncertainty since, in some cases, we cannot be sure if we sampled the same location as that used for the compositional data. We plan to investigate variations in TL properties for a given flow in the future.

The trends in the data in Figure 12 could be interpreted as follows: (1) young rocks have highly variable sensitivity, and (2) older rocks have a plateau level (around 1.5 in the figure) where the same sensitivity is produced at all ages. This might be consistent with Figure 9 in which glass has disappeared in samples >20–50 ka and it is the crystallization of glass that is giving the age relationship. This is certainly a possibility. However, also indicated in Figure 12 are the normative anorthite values. Six of the eight <20 ka samples cluster with TL sensitivity values lower than the regression line, and five of them have low An values (24–35 mol %); the exception is Hell's Half Acre. Low anorthite should cause high TL signals. While two (or more) trends are certainly possible, it seems more likely that our correction procedure is overcorrecting for composition, but on the basis of present information, there is no justification for changing it. It might be that our correction procedure is too simplistic and does not allow for the fact that there might be more than one type of feldspar present, for instance.

In Figure 13 we compare the TL sensitivity with the modal abundance of feldspar, in the form of both phenocrysts and microlites. Plots of TL sensitivity against modal abundance phenocrysts or microlites show no correlations. In Figure 13 there is no correlation between TL sensitivity and plagioclase abundance until the TL data are corrected for the composition of the plagioclase when a weak correlation ($R^2 = 0.53$) is

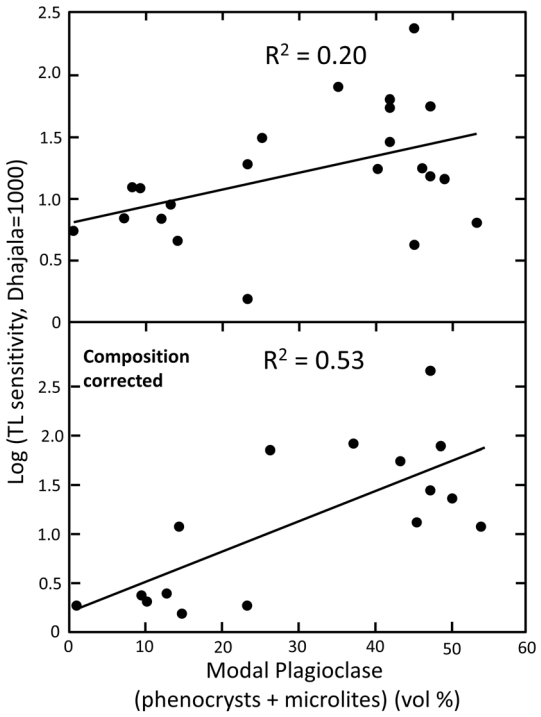

Figure 13. Plot of the log of the TL sensitivity against modal abundance of plagioclase as phenocrysts and microlites. There is no correlation when the raw TL data are used, but when the TL data are corrected for composition, there is a weak correlation. The weakness of this correlation suggests that feldspar is present in a third component. Analytical uncertainties have not been shown to simplify the figure but are a few times the sizes of the symbols.

observed. This plot should be trivial, since we know that feldspar is the phase that luminesces. What is significant is that the correlation is so weak and points to the presence of a third phase of feldspar which we hypothesize in among the secondary feldspar. Since the amount of this third component increases with time, it will only add scatter to Figure 13.

4.4. Induced TL and Weathering of Basalts

The vulnerability of the different phases in basalts to weathering varies, although the details depend on a number of factors like bulk composition [*Colman*, 1981; *Eggleton et al.*, 1987; *Nesbitt and Wilson*, 1992]. Most stable under most conditions are the opaque phases, such as titanomagnetites, which are often found surviving in the most severely altered weathering rind. Next in stability are the pyroxene and plagioclase, although this depends strongly on their composition. Most susceptible to alteration are the glass and olivine. In line with this, according to *Colman* [1981], the relative elemental mobilities in the rinds are

$$\text{Ca} > \text{Na} > \text{Mg} > \text{Si} > \text{A1} > \text{K} > \text{Fe} > \text{Ti}$$

although other authors propose slightly different sequences.

The rate of weathering depends on grain size, fracturing, and chemical zoning, and it slows down with time rather than being linear [*Colman*, 1981]. The processes of alteration include hydrolysis, leaching, oxidation, and the physical destruction of minerals. With respect to the present study, weathering has the potential to affect the TL data in two ways. First, it could add scatter to the data if individual samples were weathered to differing extents. Second, it could actually be the cause of the trends we are seeing and attributing to petrographic and mineralogical processes.

Care was taken to avoid sampling weathered material for the present study; certainly, no weathering rinds were included in our sampling. In fact, all the samples looked extremely fresh. Pending evidence to the contrary we are doubtful that weathering played a major part in causing our data to scatter.

We did observe a trend of decreasing glass abundance with age in these samples (Figure 9), as would be expected from the known weathering processes. The trend line in Figure 9 also follows the expected trend of rapid alteration followed by a rate that slows up and almost ceases, consistent with weathering. This process would also offer a means of chronometry if the rate of destruction of glass was reasonably uniform from one site to another, although we think this unlikely.

We argue that the trend in Figure 9 is not caused by weathering but by the loss of glass as it crystallizes to produce plagioclase and other phases, and the increase in TL reflects this increase in abundance of feldspar. The loss of glass by weathering would not cause an increase in induced TL because the products of glass weathering, mostly phyllosilicates, are not luminescent. In fact, *Sears et al.* [1991] identified some anomalous CM chondrites, which are normally phyllosilicates and have no measureable TL signal, but metamorphism had produced trace amounts of luminescent phases in the anomalous CM chondrites. In a similar vein, we

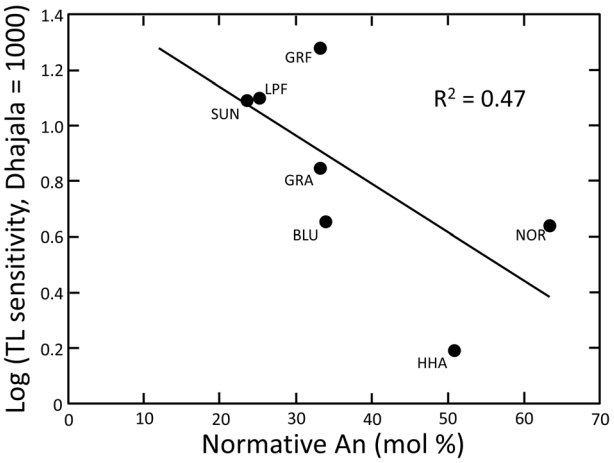

Figure 14. Plots of the logarithm of the induced thermoluminescence (Dhajala = 1000) versus normative anorthite in the plagioclase for basalts with <20 ka ages.

examined thin sections of all our samples under the microscope and, while the glass varied slightly in appearance, we did not see any evidence for phyllosilicates. We attribute the difference in the appearance of the glass to the presence of microcrystals in some samples and that weathering is not playing a part in determining the properties of our samples.

4.5. The Young (<20 ka) Samples

The spread in TL sensitivity of the <20 ka samples appears to be composition related. These samples are very similar petrographically; they are predominantly glass with vesicles and little or no phenocrysts or olivine. Microlite abundances fluctuate from 0 to over 40 vol % and might be increasing with age. There is a weak correlation between TL sensitivity and normative anorthite in the plagioclase, which is shown in Figure 14. Thus, we suspect that the spread in TL sensitivity of the <20 ka samples is reflecting differences in composition. As discussed previously, samples plotting below the regression line in Figure 13 tend to have low An values.

4.6. The Cause of the TL Sensitivity—Age Trend

May [1977] suggested that the reason for the increase in induced TL with age was due to the production of defects in the samples by radiation damage. These defects are the "traps" necessary for the luminescence process. He adopted the idea from *Liener and Geiss* [1968] and *Houtermans and Liener* [1966] who found that induced TL increased with age for meteorites which they ascribed to traps produced over time by radiation damage. *Sears* [1980] tested this idea by irradiating meteorite samples with doses of α, β, γ, and protons in excess of that received by the meteorite and failed to produce any increase in induced TL in these silicate rocks. Instead, detailed investigations showed that the apparent increase in induced TL with K-Ar age had a petrologic explanation. The apparently young samples had been shock heated, their K-Ar age reset, and their feldspar converted to glass. Subsequent studies with artificially shock-loaded feldspars confirmed this [*Hartmetz et al*., 1986]. May's suggestion that the induced TL versus age correlation is due to radiation damage is incorrect.

As explained in the introduction, we hypothesize that petrographic explanations might exist for explaining increase in induced TL with age for the basalts. We suggest that glass crystallizes and feldspar loses its Fe with time, and this increases the induced TL of the samples. It is also possible, of course, that either one of these mechanisms can be operative without the other. Maybe the induced TL is simply monitoring the diffusive loss of Fe from the feldspar just as seems to be the case with the eucrites [*Batchelor and Sears*, 1991a, 1991b]. The only evidence we have found for the increase in induced TL with age being due to glass crystallization is that the microlites might be increasing with age among the <20 ka samples, but there is no indication that this is true of the older samples. On the other hand, we find no evidence against either of these hypotheses at the present time, but clearly, the other factors affecting the TL need to be understood.

One additional possibility, suggested by Figures 9 and 12, for example, is that we are essentially dealing with a two-component system consisting of (1) the <20 ka samples which have low TL because they have little or no crystalline feldspar and (2) the >20 ka samples which have high TL because they contain abundant primary feldspar (see Figure 7). This would amount to suggesting that we are sampling a different material in our <20 ka samples from that in the >20 ka samples, so that the TL-age trend is the result of more primary feldspar in the older samples. Such might be the case with the scenario described in the sketch shown in Figure 15. In young volcanoes the glass-vesicular layers are still present, but rain fall, wind attrition, or the action of vegetation has removed this layer from older volcanoes so that we sample just the denser flows which are glass-poor, nonvesicular, and, apparently, higher in crystals such as the primary feldspar.

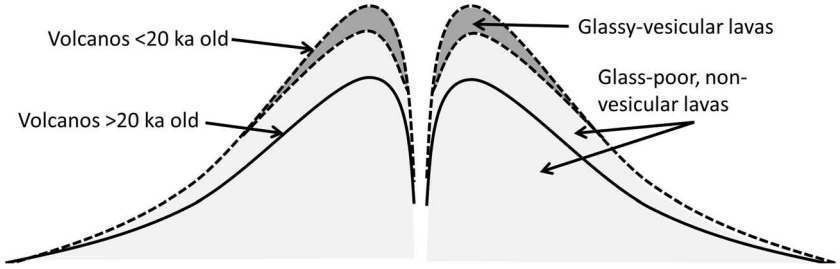

Figure 15. Schematic diagram of the aging process of a volcano that might explain some of the present data. Young volcanoes (<20 ka) have a layer of glass-rich vesicular lava that is no longer present in >20 ka volcanoes having been removed by weathering, wind action, and the effects of vegetation.

4.7. Future Studies and Applications

While we have shown that the expected correlation between induced TL and age does exist, the technique has limited value as a chronometer until the causes of the scatter are identified. This amounts to developing a better understanding of the history of basalts, of their components, such as the ratio of primary to secondary feldspars, and their thermal history, how important is cooling rate, flow rate, eruption rates, and textural changes such as the change from pahoehoe to `a`a textures. These are fundamental studies in volcanism and rheology and will not only yield new insights into the induced TL properties but will also probably gain from the insights provided by induced TL.

The theories that have evolved during this work can sometimes be tested by cathodoluminescence, electron microprobe, and other microanalytical studies. For instance changes in feldspar composition could be measured directly where the feldspars and iron diffusion profiles could be measured. However, it should be borne in mind that induced TL is an extremely sensitive technique and it is likely that the feldspar grains responsible for some of the TL trends are too small for some of these techniques. The primary purpose of the present study was to see if the trends observed by *May* [1977] were present in the Idaho field sites, but a deeper study of the behavior of basalts during and after emplacement would certainly be possible.

The effort is worth pursuing, not so much to compete with radiometric methods of age determination, although there may be instances when a nonisotopic method is helpful, but because the method has the potential for use on spacecraft. The TL-measuring equipment can easily be adapted to be low weight, low power, and low data rate, attractive specifications for use on spacecraft. Two research groups have been exploring the development of TL instruments suitable for spacecraft use, one in the USA [*Kalchgruber et al*., 2007] and one in Europe [*Bøtter-Jensen et al*., 2010], and analogous equipment using many of the components of TL apparatus have already flown on Mars missions [*Grotzinger et al*., 2012].

5. Conclusions

We attempted to see if basalts from the eastern Snake River Plain in Idaho showed the same correlation between induced TL intensity and age similar to that reported in the literature for basalts collected across the Big Island of Hawaii [*May*, 1977, 1979]. We measured the TL properties of 24 basalts varying in age from 2.2 ka to 400 ka and found a correlation, albeit with a high amount of scatter. To be a viable dating technique the scatter needs to be understood and its affects removed. We discussed the effects of variable amount of primary and secondary feldspars, the mineral producing the TL, compositional variations, and weathering. The variation in the amounts of feldspar is complicated and not completely understood, in terms of the present samples and how they were collected, and thus how this affects their induced TL properties is unclear. However, it was concluded that weathering is not important as a potential cause of scatter in our data. On the other hand, composition of the feldspar has a major influence on induced TL but can easily be allowed for. When this correction is applied, a stronger correlation between induced TL and age is observed. However, further work on the nature of lava crystallization and its relationship with TL are required to fully understand the induced TL-age correlation and the scatter.

We suggest that the TL technique could, in principle, be used for dating and that since it is low mass, low weight, and low data rate, it would be suitable for spacecraft instrumentation.

Acknowledgments
All data gathered in the execution of this work are included in this article. We appreciate funding by NASA's Solar System Exploration Research Virtual Institute via the FINESSE team, Jennifer Heldmann PI, and we appreciate the help of the FINESSE team members in collecting the samples.

References

Aitken, M. J. (1985), *Thermoluminescence Dating*, pp. 359, Academic Press, Orlando, Fla.
Aitken, M. J. (1999), *Introduction to Optical Dating*, pp. 280, Oxford Univ. Press, Oxford, U. K.
Akridge, D. G., et al. (2004), Photomosaics of the cathodoluminescence of 60 sections of meteorites and lunar samples, *J. Geophys. Res.*, *109*, E07S03, doi:10.1029/2003JE002198.
Batchelor, J. D., and D. W. G. Sears (1991a), Metamorphism of eucrite meteorites studied quantitatively using thermoluminescence, *Nature*, *349*, 516–519.
Batchelor, J. D., and D. W. G. Sears (1991b), Thermoluminescence constraints on the metamorphic, shock and brecciation history of basaltic meteorites, *Geochim. Cosmochim. Acta*, *55*, 3831–3844.
Benoit, P. H., D. W. G. Sears, and S. J. K. Symes (1996), The thermal and radiation exposure history of lunar meteorites, *Meteorit. Planet. Sci.*, *31*, 869–875.
Benoit, P. H., C. P. Hartmetz, D. J. Batchelor, S. J. K. Symes, and D. W. G. Sears (2001), The induced thermoluminescence and thermal history of plagioclase feldspars, *Am. Mineral.*, *76*, 780–789.
Berger, G. W. (1991), The use of glass for dating volcanic ash by thermoluminescence, *J. Geophys. Res.*, *96*, 19,705–19,720, doi:10.1029/91JB01899.
Bøtter-Jensen, L., K. J. Thomsen, and M. Jain (2010), Review of optically stimulated luminescence, OSL instrumental developments for retrospective dosimetry, *Radiat. Meas.*, *45*, 253–257.
Colman, S. M. (1981), Rock-weathering rates as functions of time, *Quat. Res.*, *15*, 250–264.
Drake, M. J. (2001), The eucrite/Vesta story, *Meteorit. Planet. Sci.*, *36*, 501–513.
Eggleton, R. A., C. Foudoulis, and D. Varkevisser (1987), Weathering of basalt: Changes in rock chemistry and mineralogy, *Clays Clay Miner.*, *35*, 161–169.
Fattahi, M., and S. Stokes (2003), Dating volcanic and related sediments by luminescence methods: A review, *Earth Sci. Rev.*, *62*, 229–264.
Greeley, R. (1982), The style of basaltic volcanism in the eastern Snake River Plain, Idaho, in *Cenozoic Geology of Idaho, Bur. Mines Geol. Bull.*, vol. 26, edited by B. Bonnichsen and R. M. Breckenridge, pp. 407–421.
Greeley, R., and J. S. King (1977), *Volcanism of the Eastern Snake River Plain, Idaho*, NASA, Washington D. C.
Grotzinger, J. P., et al. (2012), Mars Science Laboratory mission and science investigation, *Space Sci. Rev.*, *170*, 5–56.
Guérin, G., and G. Valladas (1980), Thermoluminescence dating of volcanic plagioclases, *Nature*, *286*, 697–699.
Haq, M., F. A. Hasan, and D. W. G. Sears (1988), Thermoluminescence and the shock and reheating history of meteorite—IV: The induced TL properties of type 4–6 ordinary chondrites, *Geochim. Cosmochim. Acta*, *52*, 1679–1689.
Hartmetz, C. P., R. Ostertag, and D. W. G. Sears (1986), A thermoluminescence study of experimentally shock-loaded oligoclase and bytownite. Proc. 17th Lunar and Planet. Sci. Conf., Part 1, *J. Geophys. Res.*, *91*, E263–E274, doi:10.1029/JB091iB13p0E263.
Heldmann, J. L., D. S. S. Lim, S. S. Hughes, S. E. Kobs-Nawotniak, W. B. Garry, G. R. Osinski, K. V. Hodges, L. Kobayashi, and A. Colaprete (2015), Overview of NASA FINESSE, field investigations to enable solar system science and exploration science and exploration results American Geophysical Union, Fall Meeting 2015, Abstract P53C-2145.
Houtermans, F. G., and A. Liener (1966), Thermoluminescence of meteorites, *J. Geophys. Res.*, *71*(14), 3387–3396, doi:10.1029/JZ071i014p03387.
Hughes, S. S., R. P. Smith, W. R. Hackett, and S. R. Anderson (1999), Mafic volcanism and environmental geology of the eastern Snake River Plain, Idaho, in *Guidebook to the Geology of Eastern Idaho: Idaho Museum of Natural History*, edited by S. S. Hughes and G. D. Thackray, pp. 143–168, Idaho Museum of Natural History, Pocatello, Idaho.
Irvine, T. N., and W. R. A. Baragar (1971), A guide to the chemical classification of the common volcanic rocks, *Can. J. Earth Sci.*, *8*, 523–548.
Kalchgruber, R., S. W. S. McKeever, M. W. Blair, E. R. Benton, and D. K. Reust (2007), A prototype instrument for in situ luminescence dating of sediments on Mars Seventh International Conference on Mars, 3074, Abstract.
Kuntz, M. A. (1992), A model-based perspective of basaltic volcanism, eastern Snake Rover Plain, Idaho, in *Regional Geology of Eastern Idaho and Western Wyoming*, *Geol. Soc. Am. Mem.*, vol. 179, edited by P. K. Link, M. A. Kuntz, and L. B. Platt, Geol. Soc. Am., Boulder, Colo.
Kuntz, M. A., E. C. Spiker, M. Rubin, D. E. Champion, and R. H. Lefebvre (1986), Radiocarbon studies of latest Pleistocene and Holocene lava flows of the Snake River Plain, Idaho; data, interpretations, *Quat. Res.*, *25*, 163–176.
Kuntz, M. A., H. R. Covington, and L. J. Schorr (1992), An overview of basaltic volcanism on the eastern Snake River Plain, Idaho, in *Regional Geology of Eastern Idaho and Western Wyoming*, *Geol. Soc. Am. Mem*, vol. 179, edited by P. K. Link, M. A. Kuntz, and L. B. Platt, pp. 227–267.
Kuntz, M. A., D. E. Owen, D. E. Champion, P. B. Gans, S. C. Smith, and C. Brossy (2004), Geology of the Craters of the Moon 30′ × 60′ map area and new perspectives on basaltic volcanism of the eastern Snake River Plain, Idaho, in *Geological Field Trips in Southern Idaho, Eastern Oregon, and Northern Nevada*, edited by K. M. Haller and S. H. Wood, pp. 134–153, USGS Open File Report 2004-1222, U.S Geol. Surv., Reston, Va.
Kuntz, M. A., B. Skipp, D. E. Champion, P. B. Gans, D. P. Van Sistine, and S. R. Snyders (2007), Geologic map of the Craters of the Moon 30′ × 60′ quadrangle, Idaho U.S. Geological Survey Scientific Investigations Map 2969, 64-p. pamphlet, 1 plate, scale 1:100,000.
Lalou, C., D. Nordemann, and J. Labyrrie (1970), Etude préliminaire de la thermoluminescence de la meteorite Saint-Severin. Compt. Rendus de l'Acad. Sci., Paris Ser. D 270.
Liener, A., and J. Geiss (1968), Thermoluminescence measurements on chondritic meteorites, in *Thermoluminescence of Geological Materials*, pp. 559–582, Academic Press, London.
May, R. J. (1977), Thermoluminescence dating of Hawaiian alkalic basalts, *J. Geophys. Res.*, *82*, 3023–3029, doi:10.1029/JB082i020p03023.
May, R. J. (1979), Thermoluminescence dating of Hawaii basalt Geol. Surv. Prof. Paper 1095.
McKinlay, A. F. (1981), *Thermoluminescence Dosimetry*, pp. 180, Adam Hilger, Bristol, U. K.
McSween, H. Y., et al. (2013), Dawn; the Vesta-HED connection; and the geologic context for eucrites, diogenites, and howardites, *Meteorit. Planet. Sci.*, *48*, 2090–2104.
Nesbitt, H. W., and R. E. Wilson (1992), Recent chemical weathering of basalts, *Am. J. Sci.*, *292*, 740–777, doi:10.2475/ajs.292.10.740.
NPS (2015). [Available at https://www.nps.gov/crmo/learn/historyculture/astronauts.htm.]
Pilleyre, T., M. Montret, J. Fain, D. Miallier, and S. Sanzelle (1992), Attempts at dating ancient volcanoes using the red TL of quartz, *Quat. Sci. Rev.*, *11*, 13–17.
Robert, B., A. Harris, L. Gurioli, E. Médard, A. Sehlke, and A. G. Whittington (2014), Textural and rheological evolution of basalt flowing down a lava channel, *Bull. Volcanic*, *76*, 824.
Rodgers, D. W., S. P. Long, N. McQuarrie, W. D. Burgel, and C. F. Hersley (2006), Geologic map of the Inkom quadrangle, Bannock County, Idaho Idaho Geological Survey Technical Report 06-2, 1:24,000, 2 sheets.

Sears, D. W. (1980), Thermoluminescence of meteorites; relationships with their K-Ar age and their shock and reheating history, *Icarus*, *44*, 190–206.
Sears, D. W. G. (2015), Induced thermoluminescence dating of basalts, *Ancient TL*, *33*, 15–19.
Sears, D. W. G., J. Lu, B. D. Keck, and J. D. Batchelor (1991), Metamorphism of CO and CO-like chondrites and comparisons with type 3 ordinary chondrites, *Proc. NIPR Symp. Antarct. Meteor.*, *4*, 1745–1805.
Sears, D. W. G., K. Ninagawa, and A. K. Singhvi (2013), Luminescence studies of extraterrestrial materials: Insights into their recent radiation and thermal histories and into their metamorphic history, *Chem. Erde*, *73*, 1–37.
Sears, D. W., and S. A. Durrani (1978), Thermoluminescence and the K-Ar age of meteorites, *Meteoritics*, *13*, 632–633.
Sears, D. W., J. N. Grossman, C. L. Melcher, L. M. Ross, and A. A. Mills (1980), Measuring the metamorphic history of unequilibrated ordinary chondrites, *Nature*, *287*, 791–795.
Sehlke, A., A. Whittington, B. Robert, A. Harris, L. Gurioli, and E. Médard (2014), Pahoehoe to `a`a transition of Hawaiian lavas: An experimental study, *Bull. Volcanol.*, *76*, 876.
Shoemaker, E. M. (1983), Asteroid and comet bombardment of the Earth, *Annu. Rev. Earth Planet. Sci*, *11*, 461–494.
Staires, D. A. (2008), Assessing the viability of carbon dioxide sequestration in eastern Snake River Plain basalts, southern Idaho MS thesis, Idaho State Univ.
Sutton, S. R. (1985), Thermoluminescence measurements on shock-metamorphosed sandstone and dolomite from Meteor Crater Arizona. I—Shock dependence of thermoluminescence properties. II. Thermoluminescence age of Meteor Crater, *J. Geophys. Res.*, *90*, 3683–3700, doi:10.1029/JB090iB05p03683.
Templer, R. H. (1986), The localised transition model of anomalous fading, *Radiat. Prot. Dosim.*, *17*, 493–497.
Visocekas, R. (1985), Tunneling radiative recombination in labradorite: Its association with anomalous fading of thermoluminescence, *Nucl. Tracks Radiat. Meas.*, *10*, 521–529.
Wintle, A. G. (1973), Anomalous fading of thermoluminescence in mineral samples, *Nature*, *245*, 143–144.